J. Braz. Chem. Soc., Vol. 18, No. 3, S1-S5, 2007.
Printed in Brazil - ©2007 Sociedade Brasileira de Química
0103 - 5053 $6.00+0.00

Study of the Inversion Reaction of the Lactonic Fusion on Eremanthine Derivatives

José C. F. Alves* and Edna C. Fantini†

Departamento de Química, Instituto de Ciências Exatas, Universidade Federal Rural do Rio de Janeiro, 23890-970 Seropédica-RJ, Brazil

This supplementary material displays some stereochemical aspects of the lactonic fusion inversion presented in the main text of the article.

After opening the lactonic ring on starting materials with *trans* fusion in basic medium, followed by mesylation stage, the carboxylates can present themselves in different conformations as rotamers (Scheme S1). In order to compare the relative stabilities of the starting materials **8-13**, their correspondent reactive carboxylates (mesylates at C-6 position) and products with stereochemical inversion at the alkoxy carbon, we elaborated Table S1 containing the steric energies for these conformers. We used the MM2 program and then the three-dimensional structures of carboxylates from the models **8-13** in Table S1, displaying less steric interactions (Figures S1-9). After data analysis (shown in Table S1 and three-dimensional structures of carboxylates), we can assume:

(*i*) all conformers with less steric interactions of the opened lactonic rings, marked with asterisk in Table S1, have smaller steric energies than their respective substrates with *trans* lactonic fusion;

(*ii*) the two epimers **32a-b** have less steric interactions than their correspondent substrates **8a-b**. Such fact, associated with the favorable geometry of the carboxylates to nucleophylic attack on C-6 positions, observed in their three-dimensional structures (Figures S1-2), should have contributed to the better conversion rate of products with *cis* fusion (**32a-b**);

(*iii*) for the model **9**, the steric interactions on the conformers with *cis* lactonic fusion (**34a-c**) are larger than those of the respective substrates with *trans* fusion (**9a-c**), so that the reaction yielding products with configuration inversion on C-6 position should be disfavored, and this must have contributed for the lower conversion rate of epimeric products **34a-c**;

(*iv*) in model **10**, the steric interactions of epimer **36** are smaller than those of the substrate, however the boat

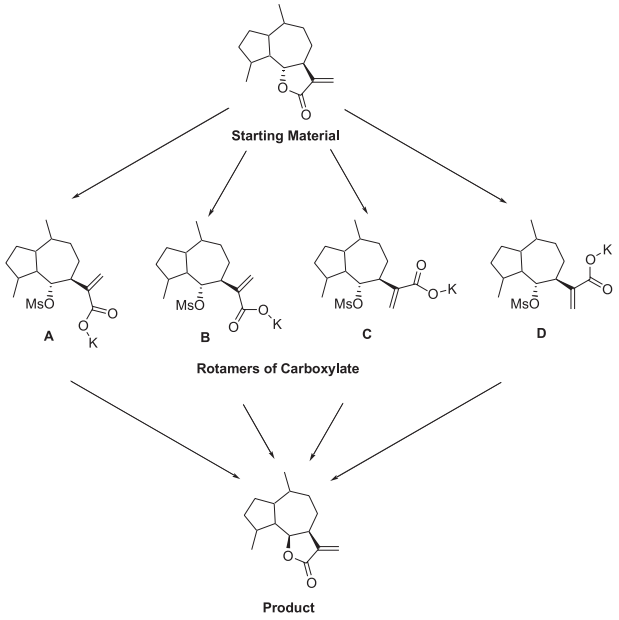

Scheme S1

(B_8) conformation of the final product is less stable than the twist-chair (TC_8) conformation of the initial substrate (Table 6 in the main text). Such fact should disfavor the formation of product **36,** leading to a larger proportion of product with *trans* lactonic fusion in relation to one with *cis* lactonic fusion;

(*v*) among the models submitted to conditions of lactonic fusion inversion, the carboxylate derived from allylic acetate **11** was the one which presented less steric interactions (Table S1). As this intermediate has few steric interations, the intermolecular nucleophylic substitution must have been favored to generate polymeric chains formation;

(*vi*) concerning model **12**, the steric interations between substrate and epimeric product (**40**) are similar. However, conformation changes between substrate (C_5) and product (C_7) (Table 6 in the main text) should be possibilities that disfavor the product formation with inversion of configuration on C-6 position;

(*vii*) the steric interactions on product **28** with *cis*

*e-mail: alvesjcf@yahoo.com.br
† Deceased in 1993

Table S1. Steric energies for starting materials, rotamers of carboxylates (**A**, **B**, **C**, **D**) and products of the reactions of lactonic fusion inversion of models **8-13**

Starting Materials	Steric Energies (kcal mol^{-1})				
	Rotamers of Carboxylates[a]				Products
	A	B	C	D	
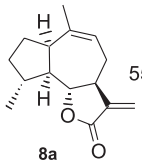 **8a**	55.542	40.701*	43.066	50.299	53.165	39.200 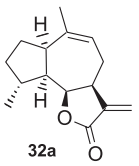 **32a**
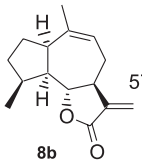 **8b**	57.985	45.109*	47.555	54.315	53.645	39.044 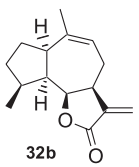 **32b**
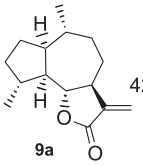 **9a**	42.403	43.669	37.082*	44.239	51.276	45.849 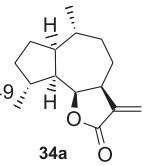 **34a**
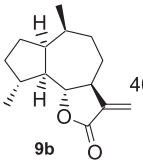 **9b**	40.628	41.170	34.126*	43.098	50.072	44.565 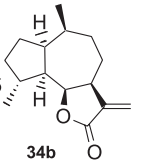 **34b**
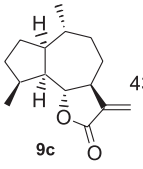 **9c**	43.182	48.023	38.710*	42.930	46.006	45.797 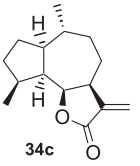 **34c**
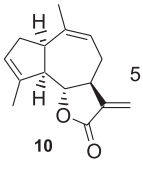 **10**	51.798	52.637	46.693*	47.951	51.294	35.302 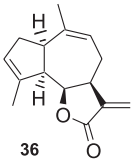 **36**
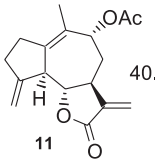 **11**	40.424	34.522	27.437*	33.256	41.105	41.541 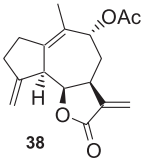 **38**
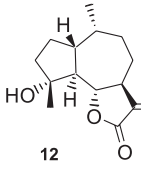 **12**	44.986	35.064	34.897*	39.703	48.308	44.594 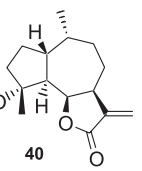 **40**
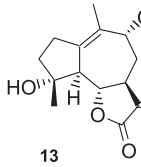 **13**	43.254	39.163	32.300*	37.032	43.221	46.455 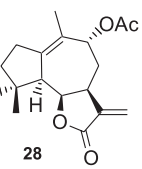 **28**

[a]Rotamers with lower energies are marked with asterisk

lactonic fusion are higher than the ones on substrate **13**. However, model **13** and its correspondent epimer **28** have the same conformations at the seven-membered ring (C_7) (Table 6 in the main text), so that, there is no process of conformational interconversion. This factor must have favored the best result obtained by this substance during the lactonic inversion reaction in relation to other models evaluated in this study.

Qualitative graphics correlating steric energy (SE) with the coordinate of the lactonic inversion reaction to the substrates with *trans* lactonic fusion (**A**), reactive intermediate mesylates (**B**) and products with *cis* lactonic fusion (**C**) (Scheme S2) for the models **8-13** are depicted in Figures S10-12.

An intriguing result was obtained in the ^{1}H NMR spectrum of crude product from the reaction of lactonic fusion inversion of model **8** (Table 4 - Exp. 1, in the main text). After analysis of this spectrum we verified atypical values of chemical shifts for the hydrogens H-13 (deshielded) and H-9 (shielded) for the compounds **32,** not exhibited before in eremanthine derivatives. After analysis of three-dimensional structures of compounds **32a-b** with *cis* lactonic fusion (Figures S14-15), we verified space proximity of hydrogens H-13 with the deshielding area of double bond C9-C10 and the proximity of hydrogen H-9 with the shielding area of α-methylene-γ-lactone. The comparison of three-dimensional structures of compounds **32a-b** (Figures S14-15), that have double bond at C9-C10 and *cis* lactonic fusion, with the similar compound 6-*epi*-isoeremanthine (**36**) that differs from **32a-b** only in the unsaturation degree at C3-C4 (Figure S13), contributed to confirm this atypical data of ^{1}H NMR obtained with these compounds. In the three-dimensional structure of compound **36** (Figure S13) we verified that there is no space proximity of hydrogens H-9 and H-13 with the shielding/deshielding areas of double bonds mentioned for compounds **32a-b**. These conformational differences observed in the three-dimensional structures of the mentioned compounds must be the cause of atypical results obtained in their ^{1}H NMR spectra.

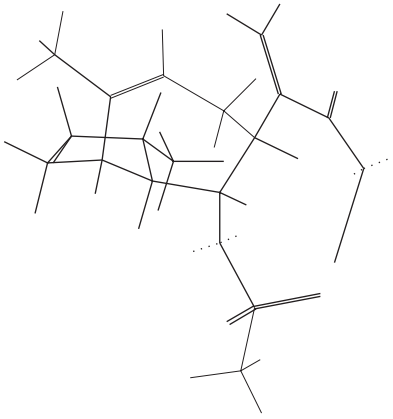

8a-A

Figure S1. Three-dimensional structure of reactive carboxylate (mesylate at C-6 position) of model **8a** with less steric interactions.

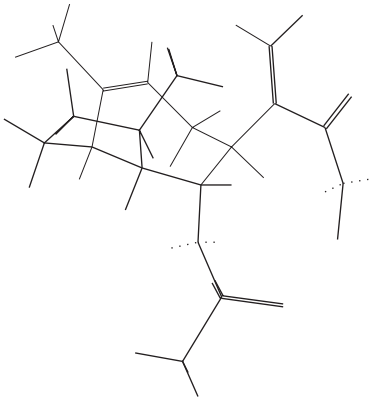

8b-A

Figure S2. Three-dimensional structure of reactive carboxylate (mesylate at C-6 position) of model **8b** with less steric interactions.

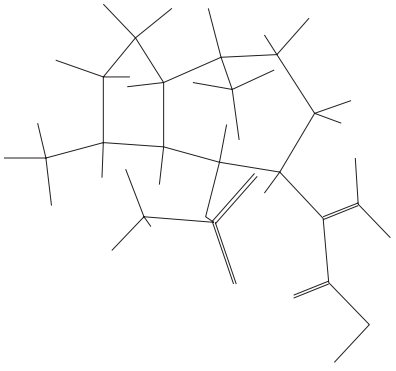

9a-B

Figure S3. Three-dimensional structure of reactive carboxylate (mesylate at C-6 position) of model **9a** with less steric interactions.

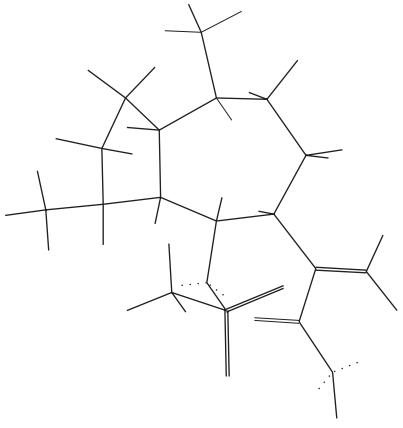

9b-B

Figure S4. Three-dimensional structure of reactive carboxylate (mesylate at C-6 position) of model **9b** with less steric interactions.

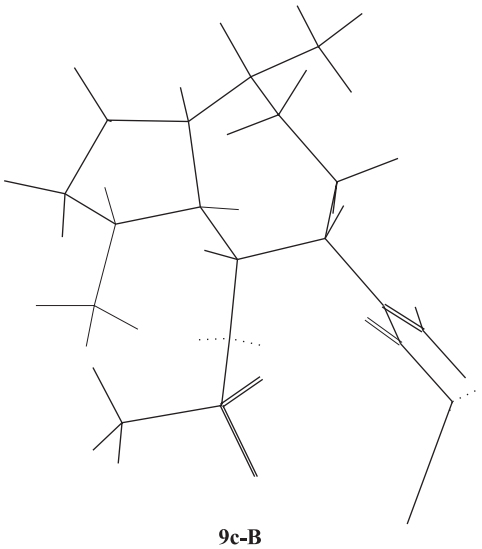

9c-B

Figure S5. Three-dimensional structure of reactive carboxylate (mesylate at C-6 position) of model **9c** with less steric interactions.

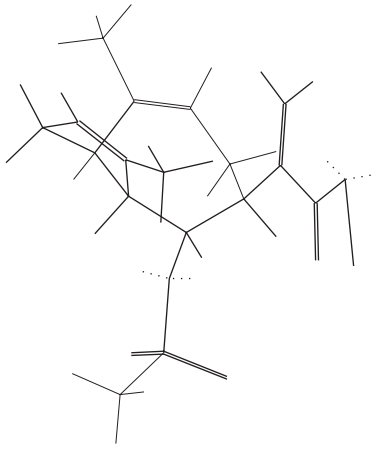

10-B

Figure S6. Three-dimensional structure of reactive carboxylate (mesylate at C-6 position) of model **10** with less steric interactions.

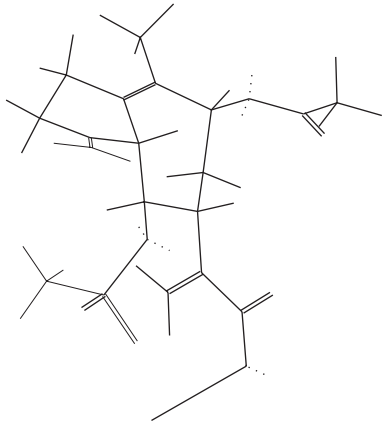

11-B

Figure S7. Three-dimensional structure of reactive carboxylate (mesylate at C-6 position) of model **11** with less steric interactions.

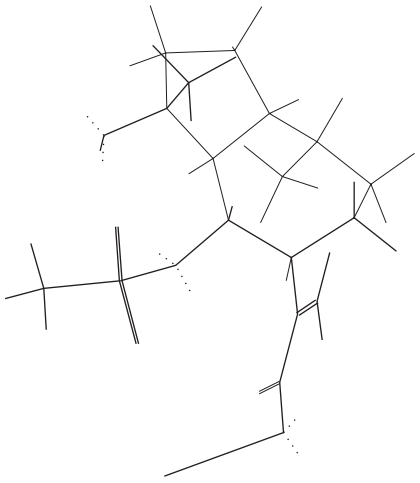

12-B

Figure S8. Three-dimensional structure of reactive carboxylate (mesylate at C-6 position) of model **12** with less steric interactions.

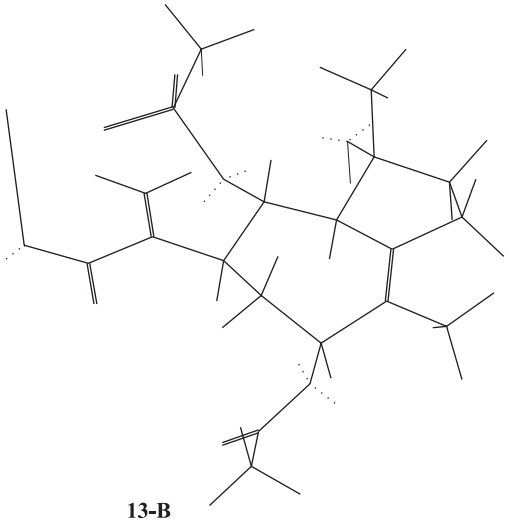

13-B

Figure S9. Three-dimensional structure of reactive carboxylate (mesylate at C-6 position) of model **13** with less steric interactions.

General Reaction

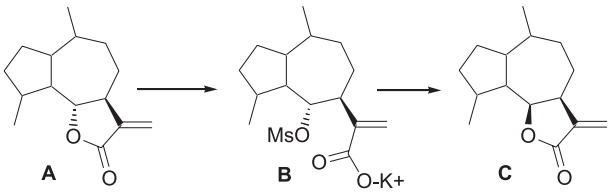

Scheme S2

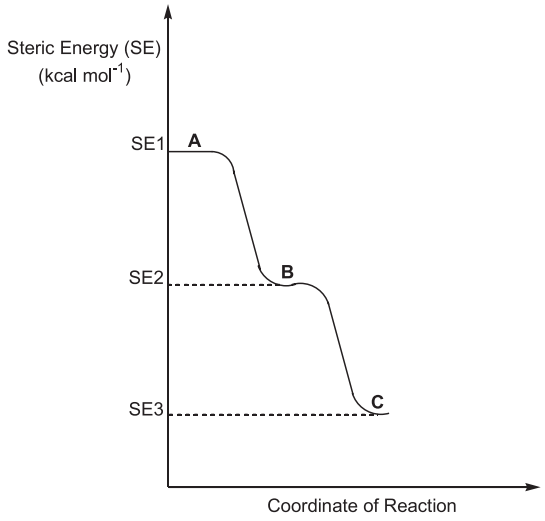

Figure S10. Qualitative graphic of steric energy (SE) versus coordinate of reaction for models **8a-b** and **10**.

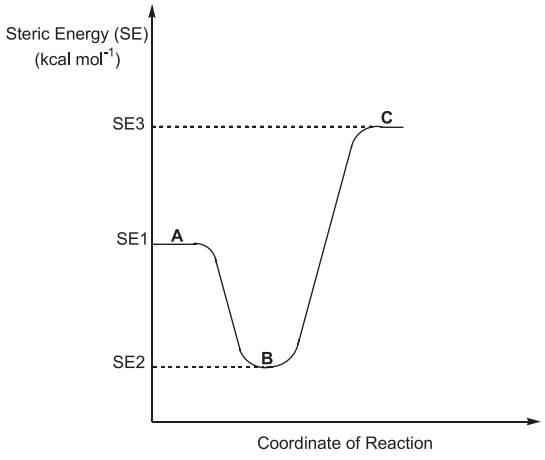

Figure S11. Qualitative graphic of steric energy (SE) versus coordinate of reaction for models **9a-c**, **11** and **13**.

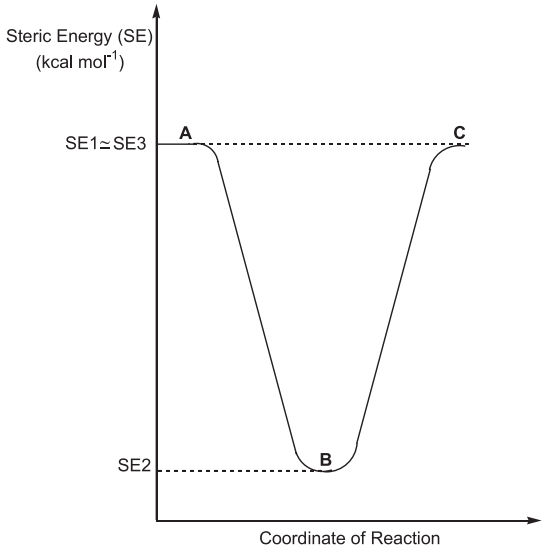

Figure S12. Qualitative graphic of steric energy (SE) versus coordinate of reaction for model **12**.

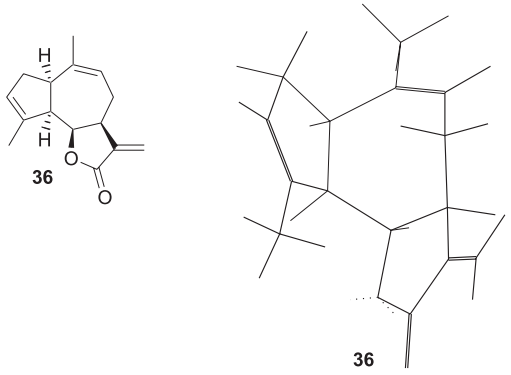

Figure S13. Three-dimensional structure of 6-*epi*-isoeremanthine (**36**).

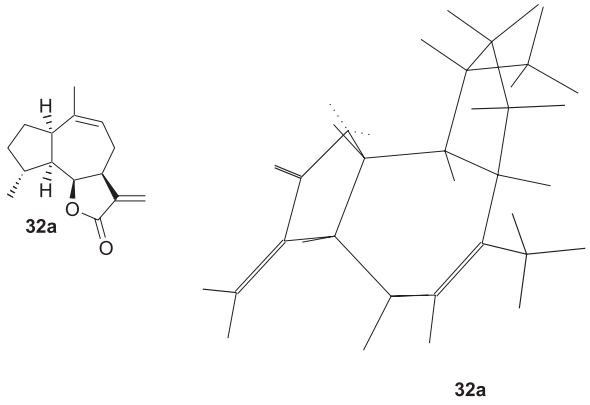

Figure S14. Three-dimensional structure of compound **32a**.

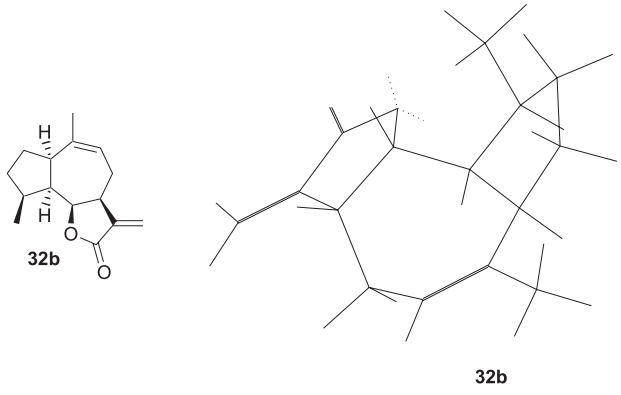

Figure S15. Three-dimensional structure of compound **32b**.